Contribution from the School of Chemistry and Molecular Science, University of Sussex, Brighton BN1 9QJ, U.K., and Department of Chemistry, University of Illinois at Chicago, Chicago, Illinois 60680

Magnetochemistry of the Tetrahaloferrate(III) Ions. 1. Crystal Structure and Magnetic Ordering in Bis[4-chloropyridinium tetrachloroferrate(III)]-4-Chloropyridinium Chloride and Bis[4-bromopyridinium tetrachloroferrate(III)]-4-Bromopyridinium Chloride

Jalal A. Zora,[1a] K. R. Seddon,[1a] Peter B. Hitchcock,[1a] Carol B. Lowe,[1b] Danny P. Shum,[1b] and Richard L. Carlin*[,1b]

Received December 14, 1989

A novel yellow salt of stoichiometry $[4\text{-Cl(py)H}]_3Fe_2Cl_9$ (where 4-Cl(py)H is 4-chloropyridinium, C_5H_6NCl) was shown by X-ray crystallography [monoclinic lattice; space group $P2_1/n$, a = 14.736 (3) Å, b = 13.923 (3) Å, c = 14.740 (3) Å, β = 92.01 (2)°, Z = 4, $R(F_o)$ = 0.054 for 2719 independent reflections with $|F^2| > \sigma(F^2)$] to contain two slightly distorted tetrahedral $[FeCl_4]^-$ anions [$\bar{r}$(FeCl) = 2.179 Å], one chloride anion, and three $[4\text{-Cl(py)H}]^+$ cations in the formula unit, all three cations being hydrogen bonded to the single chloride anion [$\bar{r}$(H···Cl) = 2.15 Å]. Magnetic susceptibility measurements on single crystals show that the $S = {}^5/_2$ material orders as a canted antiferromagnet at 2.73 (1) K. Replacement of the $[4\text{-Cl(py)H}]^+$ cation with its larger 4-bromo analogue, $[4\text{-Br(py)H}]^+$, yields an isomorphous material that orders at 2.34 (1) K. The magnetic phase diagrams of both salts have also been determined. For $2[4\text{-Cl(py)H}][FeCl_4]\cdot[4\text{-Cl(py)H}]Cl$, the bicritical point is at 2.40 K and 7.0 kOe, and $H_{SF}(0)$ = 5.5 kOe; with $H_c(0)$ = 56 kOe, $\alpha = H_A/H_E = 1.9 \times 10^{-2}$. For $2[4\text{-Br(py)H}][FeCl_4]\cdot[4\text{-Br(py)H}]Cl$, the bicritical point is at 2.24 K and 4.2 kOe and $H_{SF}(0)$ = 3.0 kOe; with $H_c(0)$ = 42 kOe, $\alpha = 1.0 \times 10^{-2}$. Both salts behave approximately as $S = {}^5/_2$, 3D Heisenberg antiferromagnets.

Introduction

The observed occurrence of canted antiferromagnetic ordering, with its almost-antiparallel magnetic moment alignment, in insulating compounds of the transition metals is still uncommon. Moreover, the ground rules for constructing a material that exhibits this phenomenon are not at all clear, at least from the practical point of view of a synthetic chemist. Magnetic properties and facile syntheses of two new double salts, bis[4-chloropyridinium tetrachloroferrate(III)]-4-chloropyridinium chloride, $2\text{-}[4\text{-Cl(py)H}][FeCl_4]\cdot[4\text{-ClpyH}]Cl$, and bis[4-bromopyridinium tetrachloroferrate(III)]-4-bromopyridinium chloride, $2[4\text{-Br(py)H}][FeCl_4]\cdot[4\text{-Br(py)H}]Cl$ are reported here, along with the crystal structure analysis of the former. Both salts are canted antiferromagnets ($S = {}^5/_2$), are members of a large series of tetrahaloferrates(III) that exhibit unusual magnetic behavior, and are being intensively studied.[2] This appears to be the first report of canted antiferromagnetism in a coordination compound of the S-state ion, iron(III).

There are many compounds of stoichiometry $A_3M_2X_9$ known, where A is typically an alkali-metal ion, M may be a variety of transition metals, and X may be fluoride, chloride, or bromide.[3,4] Many of these compounds contain the dimeric $[M_2X_9]^{3-}$ ion, such as those in which the quasi-octahedral metal ion is chromium, molybdenum, or tungsten,[5] and possess the structure $[X_3M(\mu\text{-}X)_3MX_3]^{3-}$. On the other hand, it is interesting that compounds of iron(III) known which have this stoichiometry have been shown to contain the discrete tetrahedral $[FeCl_4]^-$ ion instead.[6,7]

Experimental Section

Synthesis of Bis[4-chloropyridinium tetrachloroferrate(III)]-4-Chloropyridinium Chloride. Iron(III) chloride (0.163 g, 1.0 mmol) and 4-chloropyridinium chloride (0.3 g, 2.0 mmol) were each dissolved in water (5 cm³) separately and then mixed together. Aqueous hydrochloric acid (5 cm³; 4 M) was added to the mixture, which was then allowed to stand at room temperature for 10 days. The yellow faceted crystals were then collected by filtration and dried in vacuo. Anal. Calcd for $C_{15}H_{15}Cl_{12}Fe_2N_3$: C, 23.26; H, 1.95; Cl, 54.94; Fe, 14.42; N, 5.43. Found: C, 23.37; H, 1.91; Cl, 54.98; Fe, 14.18; N, 5.34.

Synthesis of Bis[4-bromopyridinium tetrachloroferrate(III)]-4-Bromopyridinium Chloride. Iron(III) chloride (5.8 g, 0.036 mmol) and 4-bromopyridinium chloride (12.4 g, 0.064 mmol) were each dissolved in water (14 cm³) separately and then mixed together. Aqueous hydrochloric acid (5 cm³; 4 M) was added to the mixture, which was then allowed to stand at room temperature for 10 days. The yellow crystals, which formed as the solvent evaporated, could then be monitored and selected for size as necessary, collected by filtration, and dried in vacuo. The crystal habits of the two compounds are alike; most crystals form with well-developed square {001} faces. The material was found to be isomorphous with the 4-chloropyridinium salt by X-ray precession photography. Anal. Calcd for $C_{15}H_{15}Br_3Cl_9Fe_2N_3$: C, 19.85; H, 1.66; Br, 26.41; Cl, 35.15; Fe, 12.30; N, 4.63. Found: C, 19.04; H, 1.56; Br, 26.34; Cl, 35.62; Fe, 12.41; N, 4.45.

Table I. Crystallographic Data for $2[4\text{-Cl(py)H}][FeCl_4]\cdot[4\text{-Cl(py)H}]Cl$

chem formula: $C_{15}H_{15}C_{12}Fe_2N_3$	V = 3022.3 Å³
fw = 774.44 g/mol	Z = 4
space group: $P2_1/n$ (No. 14)	λ = 0.710 69 Å
T = 25 °C	ρ_{calcd} = 1.70 g cm⁻³
a = 14.736 (3) Å	μ(Mo Kα) = 20.45 cm⁻¹
b = 13.923 (3) Å	$R(F_o)$ = 0.054
c = 14.740 (3) Å	$R_w(F_o^2)$ = 0.051
β = 92.01 (2)°	

Determination of the Crystal Structure of $2[4\text{-Cl(py)H}][FeCl_4]\cdot[4\text{-Cl(py)H}]Cl$. A crystal of dimensions 0.25 × 0.20 × 0.15 mm was mounted in a capillary tube, and both ends were sealed to protect it from atmospheric moisture (the compound is hygroscopic). This was used for all crystallographic measurements, which were made at room temperature with graphite-monochromated Mo Kα radiation (λ = 0.710 69 Å) and an Enraf-Nonius CAD4 diffractometer. Table I contains a summary of the crystallographic data collection and analysis parameters for $2[4\text{-Cl(py)H}][FeCl_4]\cdot[4\text{-Cl(py)H}]Cl$. The space group $P2_1/n$ (No. 14, nonstandard setting) was determined unambiguously from systematic absences of $0k0$ for k odd, and $h0l$ for $h + l$ odd.

Data Collection and Processing. The intensities for $h,k,\pm l$ reflections with $2 < \theta < 25°$ were measured by the θ-2θ scan technique, with a scan width of $\Delta\theta = (1.2 + 0.35 \tan\theta)°$. The integrated intensities, I, and their variances $\sigma(I)$, were corrected for Lorentz and polarization (Lp) effects, but not for absorption. Rejection of the reflections with $|F^2| \leq \sigma(F^2)$ yielded 2719 independent structure amplitudes, which were used in all subsequent calculations.

Structure Determination and Refinement. Phase determination using MULTAN[8] revealed the coordinates for two $[FeCl_4]^-$ ions. The remaining atoms of three $[4\text{-Cl(py)H}]^+$ cations and one Cl^- anion were located from

(1) (a) University of Sussex. (b) University of Illinois at Chicago.
(2) Lammers, E.; Verstelle, J. C.; van Duyneveldt, A. J.; Lowe, C. B.; Carlin, R. L. *J. Phys. (Paris), Suppl. 12* **1988**, *49*, C8-1465.
(3) Wessel, G. J.; Ijdo, D. J. *Acta Crystallogr.* **1957**, *10*, 466.
(4) Dance, J. M.; Mur, J.; Darriet, J.; Hagenmuller, P.; Massa, W.; Kummer, S.; Babel, D. *Solid State Chem.* **1986**, *63*, 446.
(5) Darriet, J. *Rev. Chim. Miner.* **1981**, *18*, 27. Stranger, R.; Smith, P. W.; Grey, I. E. *Inorg. Chem.* **1989**, *28*, 1271.
(6) Ginsberg, A. P., Robin, M. B. *Inorg. Chem.* **1963**, *2*, 817.
(7) Kovsarnechan, M. T.; Roziere, J.; Mascherpa-Corral, D. *J. Inorg. Nucl. Chem.* **1978**, *40*, 2003.
(8) Main, P. A System for Computer Program for Automatic Solution of Crystal Structure from X-ray Diffraction Data. York University, July, 1982.

0020-1669/90/1329-3302$02.50/0

Table II. Fractional Atomic Coordinates ($\times 10^4$) for $2[4\text{-Cl(py)H}]_2[FeCl_4]\cdot[4\text{-Cl(py)H}]Cl$ with Estimated Standard Deviations Given in Parentheses

	x	y	z	U_{eq}, Å^3
Fe(1)	3326 (1)	2844 (1)	1856 (1)	58 (1)
Fe(2)	3321 (1)	2868 (1)	6311 (1)	56 (1)
Cl(1)	3277 (2)	2950 (2)	381 (1)	86 (1)
Cl(2)	3481 (2)	4298 (2)	2383 (2)	100 (1)
Cl(3)	4468 (2)	1941 (2)	2286 (2)	90 (1)
Cl(4)	2105 (2)	2157 (2)	2329 (2)	113 (2)
Cl(5)	2204 (2)	3667 (2)	6874 (2)	88 (1)
Cl(6)	3151 (2)	2733 (2)	4838 (1)	79 (1)
Cl(7)	3328 (2)	1407 (2)	6859 (1)	81 (1)
Cl(8)	4615 (1)	3555 (2)	6680 (2)	84 (1)
Cl(9)	5411 (1)	3739 (2)	4047 (2)	96 (1)
Cl(10)	8770 (2)	6092 (2)	1072 (1)	89 (2)
Cl(11)	1254 (2)	−122 (2)	6390 (2)	98 (2)
Cl(12)	381 (1)	4330 (2)	3801 (1)	67 (1)
N(1)	8128 (4)	4628 (4)	5009 (4)	69 (4)
N(2)	9087 (4)	5320 (4)	−1785 (4)	61 (4)
N(3)	716 (4)	2276 (5)	4496 (4)	72 (4)
C(2)	7433 (6)	4803 (6)	5522 (5)	71 (5)
C(3)	6585 (5)	4533 (6)	5242 (5)	72 (5)
C(4)	6454 (5)	4066 (5)	4416 (5)	58 (5)
C(5)	7202 (5)	3904 (6)	3915 (5)	72 (5)
C(6)	8031 (5)	4183 (7)	4214 (5)	79 (6)
C(7)	9397 (5)	6158 (6)	−1493 (5)	69 (6)
C(8)	9307 (6)	6420 (6)	−613 (5)	74 (5)
C(9)	8889 (5)	5796 (5)	−38 (5)	53 (4)
C(10)	8576 (5)	4938 (5)	−351 (5)	62 (4)
C(11)	8675 (6)	4710 (6)	−1239 (5)	72 (5)
C(12)	711 (5)	2441 (6)	5385 (6)	70 (5)
C(13)	890 (5)	1702 (6)	5983 (5)	66 (5)
C(14)	1041 (5)	797 (6)	5644 (5)	61 (4)
C(15)	1033 (6)	640 (6)	4731 (5)	73 (5)
C(16)	860 (6)	1394 (7)	4166 (5)	84 (6)

[a] U_{eq} is defined as one-third of the trace of the orthogonalized U_{ij} tensor.

a difference Fourier map. Refinement of non-hydrogen atoms with anisotropic temperature factors was by full-matrix least-squares techniques. Hydrogen atoms at fixed calculated positions were included in the refinement with isotropic temperature factors of $B_{iso} = 6.0$ Å^2. Refinement converged at $R = 0.054$, $R' = 0.051$. The structure solution and refinement were performed on a PDP 11/34 computer, using the Enraf-Nonius Structure Determination Package. Complex neutral-atom scattering factors[9] were used throughout. Tables of thermal parameters and structure factors are included in the supplementary material.

EPR Spectroscopy. From a single crystal of the salt of stoichiometry $[4\text{-Cl(py)H}]_3M_2Cl_9$, which was grown from a solution containing 25% In(III) and 75% Fe(III) in order to dope randomly the parent compound with the diamagnetic In(III) ion, preliminary EPR spectra were obtained. The crystal was oriented by eye on a quartz rod inserted into a goniometer, before placing it into the cavity of the IBM ER200D-SRC electron spin resonance instrument. This method enabled the collection of spectra in a plane at various known angles with respect to the starting point. Spectra were collected at 30° rotation intervals, at ambient temperature and at 100 K.

Magnetic Susceptibilities. Measurements of the *ac* susceptibility, χ, given throughout in units of emu mol^{-1} of paramagnetic ion, in the temperature range 1.1–4.2 K along the crystallographic axes were conducted in an apparatus similar to that previously described.[10,11] Once the faces were indexed by using X-rays, crystals (25–90 mg) were easily aligned by eye in the sample holder, due to the clear morphology exhibited by these compounds. Cerium(III) magnesium nitrate (CMN) was used to calibrate the data. Data at higher temperatures (up to 40 K) were obtained in another cryostat described below.

Field-Dependent Susceptibilities. The field-dependent magnetic susceptibility was measured in a commercially-obtained variable-temperature, superconducting magnet Dewar by an *ac* mutual inductance method. The scheme of this experimental apparatus is much like that previously described,[12] with a few important changes to the coil system as described here.

To increase the coil sensitivity and avoid spurious signals, both the primary and secondary coils were mounted inside the insert Dewar in order to have the smallest possible volume and to remain in the region of maximum homogeneity of the external magnetic field. Both coils were wound with number 40 copper wire on a glass tube of 9-mm o.d. and 7-mm i.d. The primary coil has 1020 turns over a length of 9.7 cm, while the secondary was mounted in two sections of 220 turns each, wound in series opposition. The lengths of the secondary are much shorter than the primary. Although the coils were not at the same temperature all the time, the effect of a coupling of the coils with the applied field can be eliminated by moving the sample holder between the centers of the secondary coils. For the data shown in this paper, a measuring field estimated to be 5 Oe, operating at a frequency of 155 Hz, was used.

Table III. Intramolecular Distances (Å) and Angles (deg) for $2([4\text{-Cl(py)H}][FeCl_4])\cdot[4\text{-Cl(py)H}]Cl$ with Estimated Standard Deviations Given in Parentheses

Fe(1)–Cl(1)	2.179 (2)	Fe(1)Cl(2')	2.178 (3)
Fe(1)–Cl(3)	2.178 (3)	Fe(1)–C6(4)	2.174 (3)
Fe(2)–Cl(5)	2.176 (3)	Fe(2)–Cl(6)	2.185 (2)
Fe(2)–Cl(7)	2.188 (2)	Fe(2)–Cl(8)	2.185 (2)
Cl(9)–C(4)	1.675 (7)	Cl(10)–C(9)	1.703 (7)
Cl(11)–C(14)	1.709 (8)	N(1)–C(2)	1.318 (10)
N(1)–N(6)	1.329 (10)	N(2)–C(7)	1.320 (10)
N(2)–C(11)	1.330 (10)	N(3)–C(12)	1.331 (10)
N(3)–C(16)	1.341 (11)	C(2)–C(3)	1.355 (11)
C(3)–C(4)	1.388 (11)	C(4)–C(5)	1.367 (11)
C(5)–C(6)	1.342 (11)	C(7)–C(8)	1.359 (11)
C(8)–C(9)	1.374 (11)	C(9)–C(10)	1.356 (10)
C(10)–C(11)	1.360 (11)	C(12)–C(13)	1.374 (11)
C(13)–C(14)	1.376 (11)	C(14)–C(15)	1.363 (11)
C(15)–C(16)	1.359 (12)		

Cl(1)–Fe(1)–Cl(2)	107.0 (1)	Cl(1)–Fe(1)–Cl(3)	109.1 (1)
Cl(1)–Fe(1)–Cl(4)	110.6 (1)	Cl(2)–Fe(1)–Cl(3)	111.3 (1)
Cl(2)–Fe(1)–Cl(4)	111.9 (1)	Cl(3)–Fe(1)–Cl(4)	107.0 (1)
Cl(5)–Fe(2)–Cl(6)	111.2 (1)	Cl(5)–Fe(2)–Cl(7)	109.1 (1)
Cl(5)–Fe(2)–Cl(8)	110.3 (1)	Cl(6)–Fe(2)–Cl(7)	106.59 (9)
Cl(6)–Fe(2)–Cl(8)	110.7 (1)	Cl(7)–Fe(2)–Cl(8)	108.8 (1)
C(2)–N(1)–C(6)	122.0 (7)	C(7)–N(2)–C(11)	121.9 (6)
C(12)–N(3)–C(16)	121.4 (7)	N(1)–C(2)–C(3)	120.1 (7)
C(2)–C(3)–C(4)	119.7 (7)	Cl(9)–C(4)–C(3)	120.6 (6)
Cl(9)–C(4)–C(5)	121.8 (6)	C(3)–C(4)–C(5)	117.5 (7)
C(4)–C(5)–C(6)	121.1 (7)	N(1)–C(6)–C(5)	119.6 (7)
N(2)–C(11)–C(10)	119.9 (7)	C(7)–C(8)–C(9)	118.6 (7)
Cl(10)–C(9)–C(8)	120.2 (7)	Cl(10)–C(9)–C(10)	119.7 (6)
C(8)–C(9)–C(10)	120.2 (7)	C(9)–C(10)–C(11)	119.1 (7)
N(2)–C(11)–C(10)	199.9 (7)	N(3)–C(12)–C(13)	119.7 (7)
C(12)–C(13)–C(14)	118.8 (7)	Cl(11)–C(14)–C(13)	118.7 (6)
C(11)–C(14)–C(15)	120.7 (6)	C(13)–C(14)–C(15)	120.6 (7)
C(14)–C(15)–C(16)	118.4 (8)	N(3)–C(16)–C(15)	120.9 (7)

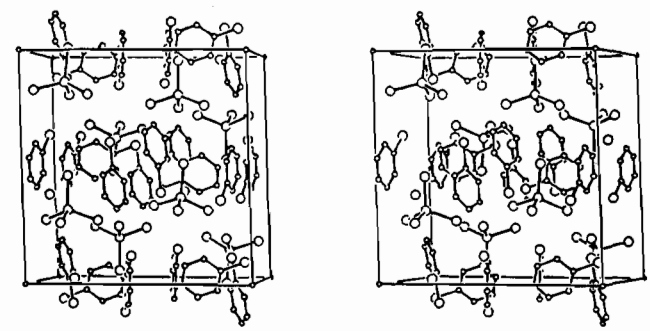

Figure 1. Unit cell of bis[4-chloropyridinium tetrachloroferrate(III)]–4-chloropyridinium chloride.

Results

Crystal Structure of $2[4\text{-Cl(py)H}][FeCl_4]\cdot[4\text{-Cl(py)H}]Cl$. Final fractional atom coordinates and bond lengths and angles (with their standard deviation in parentheses) are given in Tables II and III, respectively, for $2[4\text{-Cl(py)H}][FeCl_4]\cdot[4\text{-Cl(py)H}]Cl$.

(9) *International Tables for X-ray Crystallography*; Kynoch Press: Birmingham, England, 1974; Vol. 4.
(10) McElearney, J. N.; Losee, D. B.; Merchant, S.; Carlin, R. L. *Phys. Rev.* **1973**, *B7*, 3314.
(11) Carlin, R. L. *Magnetochemistry*; Springer-Verlag: Berlin, Heidelberg, FRG, New York, Tokyo, 1986.
(12) Carlin, R. L.; Joung, K. O.; Paduan-Filho, A.; O'Connor, C. J.; Sinn, E. *J. Phys.* **1979**, *C12*, 293.

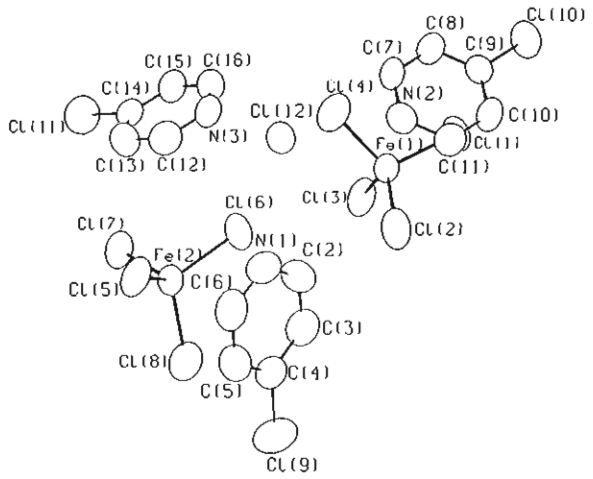

Figure 2. One labeled formula unit of 2[4-Cl(py)H][$FeCl_4$]·[4-Cl(py)-H]Cl, showing the thermal vibration ellipsoids at their 50% probability level.

Table IV. Bond Lengths with $[FeCl_4]^-$ Anions

countercation	$\bar{r}$[FeCl], Å	ref
4-chloropyridinium	2.178 (5), 2.179 (3)	*a*
pyridinium	2.16 (2)	*b*
hydroxyquinolinium	2.184 (2)	*c*
tetraphenylarsonium	2.182 (1)	*d*
2,9-dimethylphenanthrolinium	2.174 (2)	*e*
mean literature	2.175 (9)	

[a] This work. [b] James, B. D.; Millikan, M. B.; Mackay, M. F *Inorg. Chim. Acta* **1982**, *64*, L55. [c] Bottomley, G. A.; Carter, A. M.; Englehardt, L. M.; Lincoln, F. G.; Patrick, J. M.; White, A. H. *Aust. J. Chem.* **1984**, *37*, 871. [d] Cotton, F. A.; Murillo, C. A. *Inorg. Chem.* **1975**, *14*, 2467. [e] Veidis, M. V.; Witten, E. H.; Reiff, W. M. *Inorg. Chim. Acta* **1981**, *54*, L133.

The unit cell of bis[4-chloropyridinium tetrachloroferrate-(III)]-4-chloropyridinium chloride is illustrated in Figure 1, showing the eight $[FeCl_4]^-$ anions, 12 $[4\text{-Cl(py)H}]^+$ cations, and four Cl^- ions. Three (Cl···H) distances, significantly shorter than the sum of the van der Waal's radii (2.90 Å), were found between the free chloride anion and the protons on the nitrogen atoms of $[4\text{-ClpyH}]^+$:

$$Cl(12)\cdots H(N1) = 2.15\ (4)\ \text{Å} \quad (1+x, 1+y, 1+z) \quad \text{(i)}$$

$$Cl(12)\cdots H(N2) = 2.19\ (4)\ \text{Å} \quad (1+x, 1+y, \bar{z}) \quad \text{(ii)}$$

$$Cl(12)\cdots H(N3) = 2.10\ (3)\ \text{Å} \quad (x, y, z) \quad \text{(iii)}$$

Indeed, there would be some justification for describing the salt as $[[4\text{-Cl(py)H}]_3Cl]^{2+}[FeCl_4]^-_2$, at least in the solid state. Figure 2 shows one such formula unit, with thermal vibration ellipsoids for each of the labeled atoms.

The unit cell contains two unique $[FeCl_4]^-$ ions, the closest of which have a pairwise Fe···Fe separation of 6.567 Å, while the next nearest Fe···Fe contact is 7.636 Å distant. The average intraionic Fe–Cl bond lengths are 2.178 (5) and 2.179 (3) Å, comparable to other reported Fe–Cl distances, as shown in Table IV, and the Cl–Fe–Cl angles, ranging from 107.0 (1) to 111.3 (1)°, indicate slight distortions of the tetrahedra. A pictorial plot of atoms (using the atomic coordinates) contained in a pair of nearest $[FeCl_4]^-$ tetrahedra, which are nearly parallel to the unit parameter *c* of the cell, is also provided. This illustration, in Figure 3, provides a roughly quantitative view of the extent of tilting in the ions' trigonal axes, with respect to each other and to the *c* axis.

The average $\bar{r}$(CN) length of the three $[4\text{-Cl(py)H}]^+$ cations is 1.328 Å, which is in agreement with the other C–N distances, such as 1.357 (4) Å in $[4\text{-Cl(py)H}]_2[IrCl_6]$,[13] 1.33 (10) Å in $[pyH]_2[RuCl_6]$,[13] 1.343 (10) Å in $[4\text{-Cl(py)H}]_2[SnCl_6]$,[14] and also

(13) Zora, J. A. D. Phil. Thesis, University of Sussex, 1986.
(14) Gearhart, R. C.; Brill, T. B.; Welsch, W. A.; Wood, R. H. *J. Chem. Soc., Dalton Trans.* **1973**, 359.

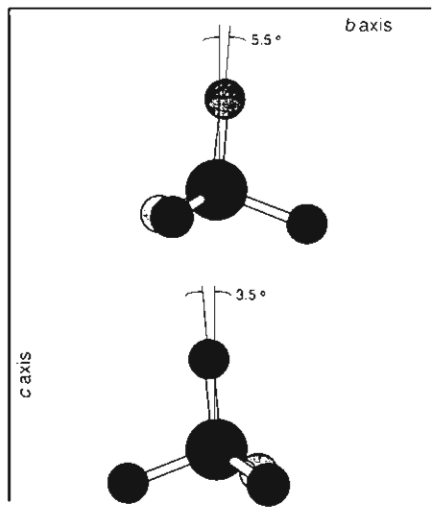

Figure 3. Nearest $[FeCl_4]^-$ pair viewed from the *bc* plane. Relative alignment of the tetrahedra with the *c* axis is shown.

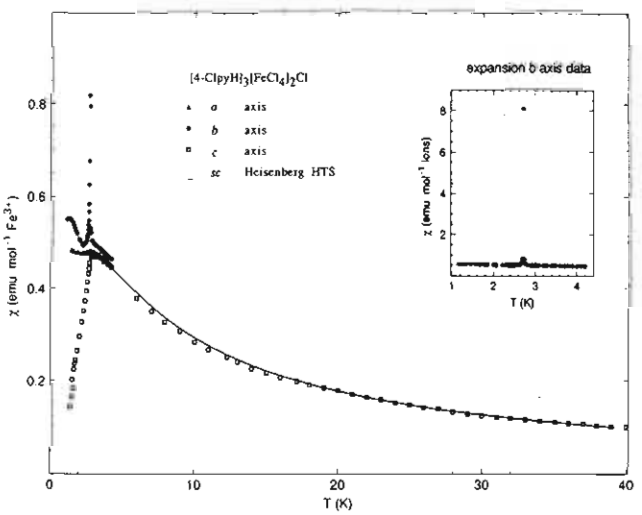

Figure 4. Single-crystal susceptibilities of bis[4-chloropyridinium tetrachloroferrate(III)]-4-chloropyridinium chloride. The data sets are identified in the inset.

in agreement with the aromatic N–C distance, 1.340 (1) Å, in pyridine.[15] Moreover, all three $[4\text{-Cl(py)H}]^+$ cations are planar, with no atom deviating from the plane by more than 0.010 Å (2σ), as shown in Table V.

Magnetic Properties of 2[4-X(py)H][$FeCl_4$]·[4-X(py)H]Cl (X = Cl or Br). The *ac* susceptibility data at zero applied field measured on a polycrystalline sample of the 4-chloropyridinium salt exhibit a sharp peak with a maximum at $T_c = 2.73$ (1) K. This is behavior characteristic usually of either a ferromagnet or a canted antiferromagnet. Subsequent measurements on oriented single crystals reveal that the material is actually a weak antiferromagnet, since the susceptibility in the *c* direction (Figure 4) is the normal parallel susceptibility of an antiferromagnet and that along *a* is the corresponding $\chi_\perp$. We note a minimum in $\chi_\perp$, occurring at $T_{min} = 2.25$ K ($T/T_c = 0.82$). Such minima have been observed previously for $RbMnF_3$ with $T/T_c = 0.78$ and also in MnF_2 with $T/T_c = 0.67$.[16] At the onset of long-range order a very narrow sharp spike due to canting of the spins on the magnetic ions is observed only in data parallel to the *b* axis, for both the in- and out-of-phase signals. The *b* axis data points shown in the figure have been limited for clarity to those below 0.85 emu mol^{-1}. The full scale of susceptibility in the vicinity of T_c is shown in the inset to Figure 4. The uppermost susceptibility

(15) Nygaard, B. B. H.; Anderson, R. *J. Mol. Spectrosc.* **1958**, *2*, 361.
(16) de Jongh, L. J.; Breed, D. J. *Solid State Commun.* **1974**, *15*, 1061.

Table V. Least-Squares Plane of $[4\text{-Cl(py)H}]^+$ in $2[4\text{-Cl(py)H}][FeCl_4]\cdot[4\text{-Cl(py)H}]Cl$[a]

plane no.	atom in plane	deviation from the plane, Å	plane no.	atom in plane	deviation from the plane, Å	plane no.	atom in plane	deviation from the plane, Å
1	N(1)	0.001	2	N(2)	−0.003	3	N(3)	0.009
	C(2)	−0.002		C(7)	−0.000		C(12)	−0.010
	C(3)	0.002		C(8)	0.001		C(13)	0.007
	C(4)	−0.001		C(9)	0.000		C(14)	−0.003
	C(5)	0.001		C(10)	−0.003		C(15)	0.001
	C(6)	−0.001		C(11)	0.005		C(16)	−0.005

[a] The dihedral angles between the planes are as follows: 1 and 2 = 54.3°; 1 and 3 = 86.3°; 2 and 3 = 140.6°. The closest interionic Cl···Cl distances (Å) are as follows: (i) Cl(2)···Cl(6) = 4.266 (x, y, z); (ii) Cl(2)···Cl(8) = 4.294 ($1-x, 1-y, 1-z$); (iii) Cl(3)···Cl(5) = 4.183 ($\bar{x}, \bar{y}, -1-z$); (iv) Cl(4)···Cl(6) = 4.037 (x, y, z); (v) Cl(4)···Cl(8) = 3.887 ($-1-x, \bar{y}, -1-z$); (vi) Cl(5)···Cl(7) = 4.331 ($x, y, 1+z$). The interionic distances between the Fe atoms are as follows: Fe(1)···Fe(1) = 7.636 Å ($x, -1+y, z$); Fe(1)···Fe(2) = 6.567 Å (x, y, z); Fe(2)···Fe(2) = 8.197 Å ($x, -1+y, 1+z$).

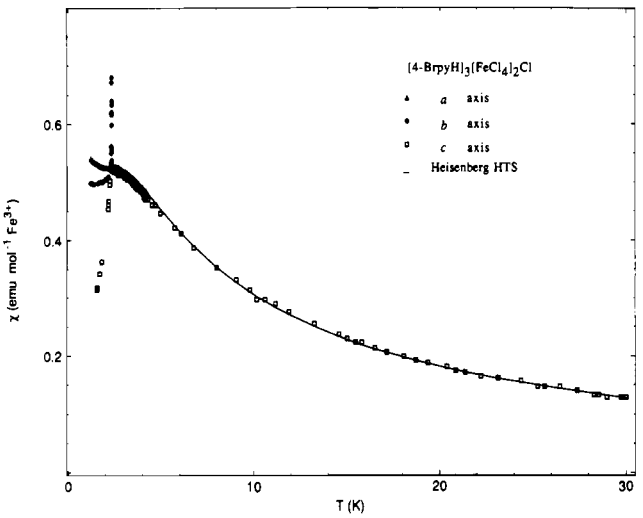

Figure 5. Single-crystal susceptibilities of bis[4-bromopyridinium tetrachloroferrate(III)]–4-bromopyridinium chloride.

point measured has a magnitude of over 8 emu mol^{-1}.

The 4-chloropyridinium salt appears from the susceptibility data to order three dimensionally. A calculated fit of the theoretical $\chi(T)$ curve for the $S = {}^5/_2$ simple cubic (sc) Heisenberg model antiferromagnet to our experimental results, shown in Figure 4, gives a g value of 2.00 and $|J|/k_B = -0.129$ K. This result is obtained from a fit to the high-temperature expansion series given by

$$1/\chi = \frac{3k_BT}{N_0g^2\mu_B^2S(S+1)}[1 + 4t^{-1} + 2.895238t^{-2} + 0.907900t^{-3} + 4.443940t^{-4} + 4.113528t^{-5} + 17.858876t^{-6} + 19.957125t^{-7} + ...] \quad (1)$$

where $t = k_BT/|J|S(S+1)$.[16] The data were fit in the temperature range 2.7–4.0 K to within approximately 3%. Deviations from the behavior as an ideal Heisenberg antiferromagnet can occur due to the presence of an anisotropy field, which has been determined from magnetic phase diagram measurements, to be described below.

We have also prepared samples of a related salt, $2[4\text{-Br(py)H}][FeCl_4]\cdot[4\text{-Br(py)H}]Cl$, which appears to have similar crystallographic and magnetic properties. Magnetic ordering is found to occur at 2.34 (1) K. The single crystal susceptibilities along the three crystallographic axes shown in Figure 5 again indicate 3-D superexchange between magnetic ions. In fitting the data, as described above for the analogous 4-chloropyridinium salt, the sc $S = {}^5/_2$ Heisenberg antiferromagnetic high-temperature series expansion was used. The best fit, which is obtained for data ranging just below T_c to 30 K, agrees to within about 2% and gives, in this case, $g = 2.004$ and $J/k_B = -0.113$ K.

Phase diagrams[11] of these two compounds were constructed from many plots of two types of magnetic susceptibility measurements: (1) susceptibility (χ) versus applied magnetic field (H) at constant temperature and (2) susceptibility versus temperature (T) at constant applied field. All measurements were made with the crystal oriented such that the applied field was parallel to the c axis.

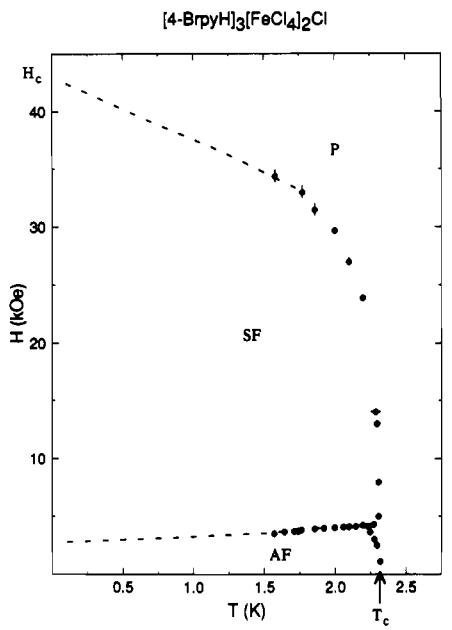

Figure 6. Phase diagram of 2[4-bromopyridinium tetrachloroferrate(III)]–4-bromopyridinium chloride: (○) susceptibility data taken at constant field with changing temperature; (●) data for which the applied field was swept at constant temperatures.

Each constant temperature plot, χ vs increasing H, indicates the first critical field transition (spin-flop field) by a sharp peak in the susceptibility as the phase boundary is crossed. The second critical field, which indicates a boundary between the spin-flop (SF) and paramagnetic (P) phases, is seen as a discontinuity in the curve. The trend in the data is that at lower temperatures, stronger applied fields are necessary to cross the boundary from SF to the P phase, while the first critical field at the AF/SF boundary was affected only slightly by the temperature below the bicritical point, where the three phases meet. Some of these plots are illustrated in the supplementary figure, Figure S1. The solid circles in the phase diagrams, seen in Figures 6 and 7, are obtained from these χ vs H plots at the temperatures implied by the plot scales. The T_c indicated on the figure is defined as the temperature at which the compound goes from the paramagnetic phase to the ordered antiferromagnetic phase at zero applied magnetic field.

From constant field plots, χ vs increasing T, a phase transition point is determined from the maximum slope in each data curve. For low constant field, (<4.2 or 7 kOe, respectively for the $[4\text{-Br(py)H}]^+$- and $[4\text{-Cl(py)H}]^+$-containing salts), the curves are very similar to zero-field susceptibility χ vs T curves. Above the bicritical point, the curves become broader; however, phase transitions remain evident as the maximum slope occurring in the data (Figure S2).

The magnetic phase diagram (the H–T plane) of $2[4\text{-Br(py)H}][FeCl_4]\cdot[4\text{-Br(py)H}]Cl$ as constructed from many of these

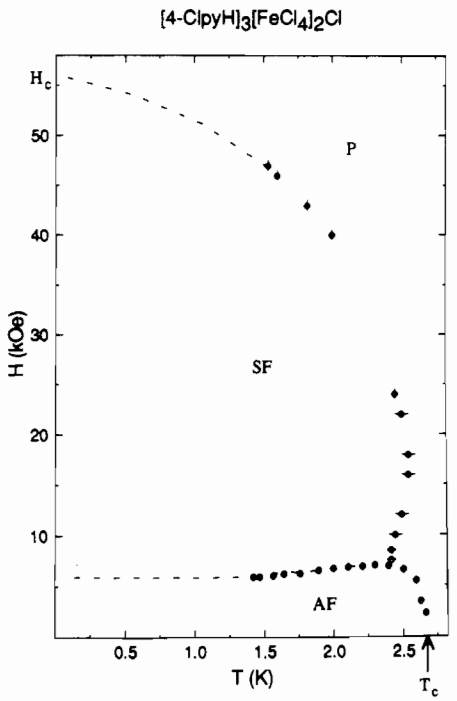

Figure 7. Phase diagram of 2[4-chloropyridinium tetrachloroferrate(III)]-4-chloropyridinium chloride: (○) $\chi(T)$, at constant H; (●) $\chi(H)$ with T constant.

susceptibility curves, is presented in Figure 6. It is typical of those reported for antiferromagnets with weak anisotropy.[11] In the Figure 6, typical error bars reflect an uncertainty in the data estimated from the value of the critical field or the location of the transition temperature. The bicritical point, where the three phases meet, is found at T_b = 2.24 K and H_b = 4.2 kOe. Taking the spin-flop field extrapolated to zero temperature as $H_{SF}(0)$ = 3 kOe and the critical field as $H_c(0)$ = 42 kOe, the anisotropy field H_A and the exchange field H_E were estimated by using the molecular field theory (MFT) approach:[11]

$$H_{SF}(0) = [2H_EH_A - H_A^2]^{1/2} \quad (2)$$

$$H_c(0) = 2H_E - H_A \quad (3)$$

The results are H_A = 215 Oe, H_E = 21 kOe, the ratio $\alpha = H_A/H_E = 1.0 \times 10^{-2}$ and $z|J|/k_B = g\mu_BH_E/2k_BS$ = 0.57 K.

The magnetic phase diagram of 2[4-Cl(py)H][$FeCl_4$]·[4-Cl(py)H]Cl, given in Figure 7, was determined in a similar fashion. The general shape of this H–T diagram is almost the same as the one for 2[4-Br(py)H][$FeCl_4$]·[4-Br(py)H]Cl with the exception that the vertical scale magnitude in the former one is about 25% higher than the latter. This trend is expected because $T_c(0)$ of 2[4-Cl(py)H][$FeCl_4$]·[4-Cl(py)H]Cl is slightly higher than $T_c(0)$ of 2[4-Br(py)H][$FeCl_4$]·[4-Br(py)H]Cl. We find T_b = 2.4 K at H_b = 7 kOe, $H_{SF}(0)$ = 5.5 kOe, and $H_c(0)$ = 56 kOe. This allows the determination that H_A = 540 Oe, H_E = 28 kOe, $\alpha = 1.9 \times 10^{-2}$, and $z|J|/k_B$ = 0.76 K.

No orientation dependence of the g values was observed in the single-crystal EPR measurements for a magnetically concentrated sample of the [4-Cl(py)H]$^+$ salt. The line shape of the spectrum is Lorentzian, and the isotropic value of g obtained is 2.02. The relative magnitudes of the EPR signal measured at room temperature and 100 K agree with the prediction of the temperature dependence of the Boltzmann population. The sample was not dilute enough in magnetic ion to obtain further characterizations; however, the direct measurement of g is an important confirmation of values obtained from fits of the susceptibility data.

Discussion

Syntheses. The iron(III) chloride, inorganic cation or organic base, and aqueous hydrochloric acid system is known to produce a range of anionic complexes, including $[FeCl_6]^{3-}$, $[FeCl_5(OH_2)]^{2-}$, and $[FeCl_4]^-$.[17] The system also has a propensity to produce double salts, making product stoichiometry an unreliable indicator of the nature of the anion. Thus, the product of stoichiometry $[MeNH_3]_4FeCl_7$ is formulated as $[MeNH_3]_3[FeCl_6]$·$[MeNH_3]$-Cl,[18] the substances $[pyH]_3Fe_2X_9$ (py = pyridine, X = Cl or Br) are formulated as 2[pyH][FeX_4]·[pyH]X,[6] and the material $[pyH]_5Fe_2Cl_{11}$ has been crystallographically characterized as 2[pyH][$FeCl_4$]·3[pyH]Cl.[19] The factors favoring the formation of one anion over another are still unclear, but the size of the cation and its ability to form strong hydrogen bonds are clearly important. The products from the iron(III) chloride, 4-halopyridinium chloride, and hydrochloric acid system analyze well for [4-X-(py)H]$_3Fe_2Cl_9$ (X = Cl or Br), despite a reaction mole ratio of 2:1 for cation:iron. The crystal structure of the 4-chloropyridinium salt (vide supra) shows that the salt contains the tetrachloroferrate(III) anion, and not the (μ-trichloro)bis[trichloroferrate(III)] anion, $[Fe_2Cl_9]^{3-}$, suggested by its stoichiometry.

Sources of Canting. Strong absorption (χ'') over the region of the sharp peak in χ' for these tetrachloroferrates(III) suggests indeed that the materials are canted antiferromagnets. It is interesting to point out that the related substance [NEt_4][$FeCl_4$], when it is cooled rapidly, orders ferromagnetically. In this case, the ferromagnetism arises because of crystal-phase transitions that the nominally antiferromagnetic material undergoes.[20] However, the observation of canted antiferromagnetism among $[FeCl_4]^-$ salts is of special interest because of the isotropic nature of the iron(III) ion.[5] Canting usually requires a degree of magnetic anisotropy in the magnetic ion[21] and is perhaps most common in cobalt(II) salts, for cobalt usually exhibits very large g value anisotropy. On the other hand, iron(III) is isoelectronic with manganese(II), and there are many examples[11] of weak ferromagnets of manganese(II). The source of canting in manganese systems has usually been ascribed to single-ion anisotropy (zero-field splitting), small as it is with manganese. Copper(II), which cannot undergo a zero-field splitting, is an ion that is nearly as isotropic as manganese(II), and canting is also found with several cupric salts. In these salts, the weak antiferromagnetic component is predicted in terms of antisymmetric superexchange interactions between ions tilted with respect to each other in the magnetic lattice.[22] Multiple sublattices for which the small ferromagnetic moments cancel effect the hidden canting, evident only from neutron diffraction experiments.

In order to discern the possible source of canting in these structures, relevant information from previous investigations of Fe(III) compounds is recalled. An EPR study of pure [NEt_4][$FeCl_4$] has been reported;[23] a g value of 2.021 (5) was observed, but no fine structure was detected. The only EPR studies of which we are aware on a dilute tetrachloroferrate(III) are those of [$P(C_6H_5)_4$][$FeCl_4$], diluted isomorphously by gallium.[24] A value of the zero-field splitting of D/k = −0.06 K is reported at 4.2 K. This is quite a small value. Dipolar terms may also contribute to the anisotropy. Indeed, it was pointed out above that the $[FeCl_4]^-$ ions occur in pairs. With 6.567 Å separating the two tetrahedra, a small anisotropic dipole interaction will likely result. Each of these effects as they pertain to this study will be considered below, with strongly symmetry-dependent antisymmetric exchange interactions emphasized.

Magnetic Model for Exchange Interactions. The Heisenberg model is the obvious choice for close comparison to these com-

(17) Nelson, S. M. In *Comprehensive Coordination Chemistry*; Wilkinson, G., Gillard, R. D., McCleverty, J. A., Eds.; Pergamon Press: Oxford, England, 1987, Vol. 4, p 217.
(18) Clausen, C. A., III; Good, M. L. *Inorg. Chem.* **1968**, *7*, 2662.
(19) James, B. D.; Millikan, M. B.; Mackay, M. F. *Inorg. Chim. Acta* **1982**, *64*, L55.
(20) Puĕrtolas, J. A.; Navarro, R.; Palacio, F.; González, D.; Carlin, R. L.; van Duyneveldt, A. J. *J. Magn. Magn. Mater.* **1983**, *31*, 1067.
(21) Moriya, T. *Phys. Rev.* **1960**, *120*, 91.
(22) Kubo, T.; Yamahaku, H. *Phys. Rev.* **1985**, *B32*, 1831.
(23) Puĕrtolas, J. A.; Orera, V. M.; Palacio, F.; van Duyneveldt, A. J. *Phys. Lett. A* **1983**, *98*, 374.
(24) (a) Deaton, J. C.; Gebhard, M. S.; Koch, S. A.; Millar, M.; Solomon, E. I. *J. Am. Chem. Soc.* **1988**, *110*, 6421. (b) Deaton, J. C.; Gebhard, M. S.; Solomon, E. I. *Inorg. Chem.* **1989**, *28*, 877.

Table VI. Exchange Constant, $|J|/k_B$ (K), Obtained by Various Methods for Some sc, $S = {}^5/_2$ Heisenberg Antiferromagnets

	$\|J\|/k_B$		
method	$[4\text{-Cl(py)H}]_3[FeCl_4]_2Cl$	$[4\text{-Br(py)H}]_3[FeCl_4]_2Cl$	$Cs_2[FeCl_5(H_2O)]^a$
fit, HTS	0.129 (3)	0.110 (3)	0.310 (5)
$\chi_{max}{}^a$	0.125 (2)	0.111 (1)	0.290 (3)
$T_c{}^a$	0.110 (1)	0.094 (1)	0.259 (2)
$T(\chi_{max})^a$	0.110 (4)	0.096 (4)	0.275 (1)
$H_E{}^b$	0.127	0.095	0.342

[a] Based on calculations of Puêrtolas et al.[25] [b] Exchange field, from the phase diagram.

pounds due to the nature of the Fe(III) ion and from the isotropic susceptibilities above T_c; however, a selection of the particular lattice model from the crystal packing is not as simple. Each Fe atom has one nearest neighbor. In addition, around the Fe(1) atoms there are four next nearest iron atoms, and two further that are about half an angstrom more distant. Ions containing Fe(2) have but two next nearest neighbors and four additional neighbors, which are about 0.8 Å beyond those. This analysis does not lead directly to the ideal sc, bcc, or fcc lattice models; therefore, it is necessary to determine the particular lattice model approximated by these compounds by a direct comparison to the susceptibility data.

Previously tabulated critical parameters given by Puêrtolas and associates for sc and bcc Heisenberg antiferromagnetic lattices[25] were used by substituting values of T_c, $T(\chi_{max})$, and χ_{max} obtained from our data into the appropriate given theoretical expression in order to evaluate the exchange parameters, $|J|/k_B$, for comparison to experimentally derived values. For the simple cubic lattice, calculations yield for $|J|/k_B$, 0.110, 0.110, and 0.125 K respectively for the salt containing 4-chloropyridinium ions and 0.094, 0.096, 0.111 K for the 4-bromopyridinium analogue. Similar analyses using the theoretical bcc values give less consistent results for $|J|/k_B$, which is an indication that the simple cubic lattice model more closely approximates the magnetic order in these systems.

In Table VI, the values of the exchange parameter, $|J|/k_B$, obtained from the HTS fit of the experimental data and sc Heisenberg $S = {}^5/_2$ antiferromagnetic model predictions are compared. Values obtained by using the high-temperature series expansion are somewhat higher than the models predict. However, the HTS expansion analysis includes only nearest-neighbor interactions, and effects of more distant neighbors may be influencing results presented here. The values of 0.127 K and 0.095 K, respectively, for $[4\text{-Cl(py)H}]_3[FeCl_4]_2Cl$ and $[4\text{-Br(py)H}]_3[FeCl_4]_2Cl$ obtained from the phase-diagram data are close to the calculated results for the sc lattice model with its six nearest neighbors. A careful analysis of the $\chi_\parallel$ zero-field data has led to the values $[T(\chi_m) - T_c]/T(\chi_m) = 0.084$ and 0.090 for 2[4-Br(py)H][$FeCl_4$]·[4-Br(py)H]Cl and 2[4-Cl(py)H][$FeCl_4$]·[4-Cl(py)H]Cl, respectively, where $T(\chi_m)$ is the temperature at which χ reaches its maximum value. These values of the above ratio are typical of those found with other three-dimensional Heisenberg antiferromagnets such as $RbMnF_3$,[16] and $Cs_2[FeCl_5(H_2O)]$,[26] and agree well with the theoretical expectation of 0.08.[16]

These results show that both 2[4-Br(py)H][$FeCl_4$]·[4-Br(py)H]Cl and 2[4-Cl(py)H][$FeCl_4$]·[4-Cl(py)H]Cl are good examples of the $S = {}^5/_2$, three-dimensional Heisenberg model antiferromagnet. In addition, values of α, or H_A/H_E, on the order of 10^{-2} (as obtained from the phase diagrams) indicate low anisotropy in the range of α's reported for $Cs_2[FeCl_5(H_2O)]$[26] and MnF_2,[27] both of which are good examples of this magnetic model system.

Sources of Anisotropy. Several other important features are to be noted from the phase-diagram data. First is the fact that the AF-P phase boundary appeared to be almost vertical; the ratio $T_b/T_c(0) = 0.96$ and 0.88 for 2[4-Br(py)H][$FeCl_4$]·[4-Br(py)H]Cl and 2[4-Cl(py)H][$FeCl_4$]·[4-Cl(py)H]Cl, respectively. A number of other weakly anisotropic antiferromagnets, such as $Cs_2[FeCl_5(H_2O)]$,[26] $K_2[FeCl_5(H_2O)]$,[28] $CuCl_2{\cdot}2H_2O$,[29] and MnF_2, behave similarly. Second, is that the derived anisotropy fields are shown to be quite small. The most important sources of the anisotropy field are single-ion or crystal-field anisotropy and dipole–dipole interactions; if zero-field splitting alone contributes, then $g\mu_B H_A = 2|D|(S - {}^1/_2)$, where D is the zero-field splitting parameter. $|D|$ was estimated to be 7 mK or 5×10^{-3} cm^{-1} and 18 mK or 1.3×10^{-2} cm^{-1} for 2[4-Br(py)H][$FeCl_4$]·[4-Br(py)H]Cl and 2[4-Cl(py)H][$FeCl_4$]·[4-Cl(py)H]Cl, respectively. The anisotropy field in similar compounds of isoelectronic Mn(II) is generally ascribed to zero-field splitting, which is usually small—on the order of 10^{-2} cm^{-1}.

Spin Canting Due to Antisymmetric Exchange, or the So-Called Dzyaloshinskii–Moriya (DM) Interaction.[17,30] The DM interaction is given by the Hamiltonian

$$H_{DM} = \sum_{ij} \vec{D}_{ij} \cdot [\vec{S}_i \otimes \vec{S}_j] \tag{4}$$

where $\vec{D}_{ij}$ is a constant vector and may be described as the antisymmetric exchange. The interaction can exist only when there is no center of inversion located halfway between the ions i and j. The order of magnitude of D can be estimated by using the relation: $|D/2J| = (g - 2)/g$. The g value used for this estimate is the one in the direction of D. The presence of the DM interaction leads to a canting of the magnetic moments. From the Curie–Weiss fit along the b axis, g_b(canting) = 2.08 is obtained for 2[4-Cl(py)H][$FeCl_4$]·[4-Cl(py)H]Cl. It is easy to show that the energy at $T = 0$ K will be minimal when the canting angle ϕ is equal to $|D/2J|$.[11,21] Using the value of g_b obtained above, we find $\phi = 0.04$ rad (2.2°). Similarly for 2[4-Br(py)H][$FeCl_4$]·[4-Br(py)H]Cl, we find $\phi = 0.036$ rad (2.0°).

Using a Hamiltonian of the form

$$H = -2J\sum \vec{S}_i \cdot \vec{S}_j + D\sum S_{jz}{}^2 + D\sum (S_{ix}S_{jy} - S_{iy}S_{jx}) + g\mu_B \vec{H} \cdot \sum \vec{S}_j \tag{5}$$

with a molecular field approximation, Moriya[31] has predicted a very sharp change in the temperature variation of the paramagnetic susceptibility close to T_c for a canted spin system. The zero-field susceptibility measured along the direction of the weak ferromagnetic moment should be given by[32-34]

$$\chi_\perp{}^{cant} = \chi_c \frac{T - T_0}{T^2 - T_c{}^2} \tag{6}$$

where

$$\chi_c = \frac{N_0 g^2 \mu_B{}^2 S(S+1)}{3k_B}$$

$$T_c = \frac{-2JzS(S+1)}{3k_B}\left[1 + \left(\frac{D}{2J}\right)^2\right]^{1/2}$$

$$T_0 = \frac{-2JzS(S+1)}{3k_B}$$

(25) Puêrtolas, J. A.; Navarro, R.; Palacio, F.; Bartolomé, J.; Carlin, R. L. *Phys. Rev. B* **1982**, *26*, 395.
(26) Paduan-Filho, A.; Palacio, F.; Carlin, R. L. *J. Phys. Lett. (Paris)* **1978**, *39*, L279.
(27) Shapira, Y.; Becerra, C. C. *Phys. Lett.* **1976**, *A57*, 483; *A58*, 493.
(28) Palacio, F.; Paduan-Filho, A.; Carlin, R. L. *Phys. Rev.* **1980**, *B21*, 296.
(29) Butterworth, G. J.; Zidell, V. S. *J. Appl. Phys.* **1969**, *40*, 1033.
(30) Dzyaloshinsky, I. *J. Phys. Chem. Solids* **1958**, *4*, 241.
(31) Moriya, T. *Phys. Rev.* **1960**, *117*, 635.
(32) Groenendijk, H. A.; van Duyneveldt, A. J.; Willett, R. D. *Physica* **1979**, *98B*, 53.
(33) Losee, D. B.; McElearney, J. N.; Shankle, G. E.; Carlin, R. L.; Cresswell, P. J.; Robinson, W. T. *Phys. Rev.* **1973**, *B8*, 2185.
(34) Joung, K. O. Thesis, University of Illinois, 1979, unpublished.

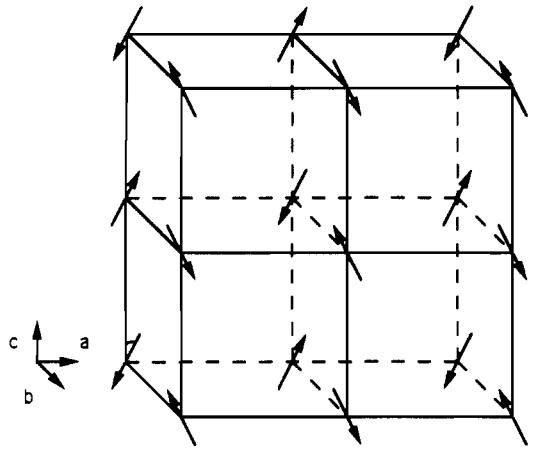

Figure 8. Possible spin configuration for 2[4-halopyridinium tetrachloroferrate(III)]-4-halopyridinium halide. The canting angle is greatly exaggerated in the drawing.

and where z is the number of nearest neighbors and S is the spin.

To avoid the usual poor prediction of the transition temperature by molecular field theory (MFT), T_c may be set to the actual transition temperature. In that case

$$\chi_{\perp}^{\text{cant}} = \chi_c \frac{T - T_c/[1 + (D/2J)^2]^{0.5}}{T^2 - T_c^2} \qquad (7)$$

A preliminary fit of this equation to 2[4-Cl(py)H][$FeCl_4$]·[4-Cl(py)H]Cl data along the canting direction was not good, partly because the data rise faster and sharper than the simple MFT predicted. Nevertheless, we obtained the fitted $g_{\perp}^{\text{cant}}$ close to 2.08 and |D/2J| equal to 0.05 rad, which is close to the value 0.04 rad as deduced from the $\Delta g/g$ calculation.

Spin Configuration. Although the detailed spin structure of these compounds will not be known until neutron diffraction studies are completed, it still is possible to postulate a reasonable picture of the spin array that is consistent with the structural and susceptibility results. These results have revealed a three-dimensional spin system. Such a spin array is shown in Figure 8, where the degree of canting, ϕ, is exaggerated for clarity. The array may be described as an almost simple cubic antiferromagnet in which the spins are coupled antiferromagnetically along all directions. As the susceptibility measurements show that the easy axis lies along the c direction and canting occurs only in the b direction, it is proposed that the spins are quantized in the c axis, but that they make an angle ϕ with the b axis of some 2°, rather than the 0° that occurs with a normal antiferromagnet. Because no weak ferromagnetic moment is detected in χ_a, the spins must lie in the bc plane, resulting in a small net moment along b.

Superexchange, as seen from these experiments, occurs in a three-dimensional network connecting the iron tetrahedra. The likely superexchange paths for these and similar compounds are explored in part 2 of this series.[35]

Acknowledgment. The work in Chicago was supported in part by the Solid State Chemistry Program of the Division of Materials Research of the National Science Foundation, under Grants DMR-8515224 and DMR-8815798. We also thank Basrah University and the Iraqi government for the award of a scholarship. Acknowledgement is made to the donors of the Petroleum Research Fund, administered by the American Chemical Society, for partial support of this research. Hau Wang at Argonne National Laboratory helped to obtain the EPR spectra.

Supplementary Material Available: Plots of (χ vs H)$_T$ (Figure S1) and (χ vs T)$_H$ (Figure S2) data curves for $C_{15}H_{15}Br_3Cl_9Fe_2N_3$ and tables of crystallographic parameters, fractional atomic coordinates for H atoms at calculated positions, and thermal parameters (6 pages); a table of structure factor amplitudes for $C_{15}H_{15}Cl_{12}Fe_2N_3$ (14 pages). Ordering information is given on any current masthead page.

(35) Lowe, C. B.; Carlin, R. L.; Loong, C.-K.; Schultz, A. J. *Inorg. Chem.*, following paper in this issue.

Contribution from the Department of Chemistry, University of Illinois at Chicago, Chicago, Illinois 60680, and Chemistry, Materials Science and Pulsed Neutron Divisions, Argonne National Laboratory, Argonne, Illinois 60439

Magnetochemistry of the Tetrahaloferrate(III) Ions. 2. Crystal Structure and Magnetic Ordering in [4-Br(py)H]$_3Fe_2Cl_{1.3}Br_{7.7}$ and [4-Cl(py)H]$_3Fe_2Br_9$. The Superexchange Paths in the $A_3Fe_2X_9$ Salts

Carol B. Lowe, Richard L. Carlin,* Arthur J. Schultz, and C.-K. Loong

Received December 14, 1989

A series of neutron diffraction investigations at 25 K are reported on single crystals of stoichiometry (4-chloropyridinium)$_3Fe_2Br_9$ and on (4-bromopyridinium)$_3Fe_2Cl_{1.3}Br_{7.7}$. The compound of stoichiometry (4-bromopyridinium)$_3Fe_2Cl_{1.3}Br_{7.7}$ is found to belong to the space group $P2_1/n$ with four formula units in the unit cell. Structural analysis shows that the iron is present as the [FeX_4]$^-$ ion (X = Cl, Br). The cell dimensions are a = 14.892 (3) Å, b = 14.184 (4) Å, c = 15.147 (4) Å, and β = 91.44 (2)°. The related compound (4-chloropyridinium)$_3Fe_2Br_9$ is found to belong to the same space group with a = 14.856 (3) Å, b = 14.066 (3) Å, c = 15.216 (3) Å, and β = 92.15 (1)°. Both materials are isomorphous with the previously reported bis[4-chloropyridinium tetrachloroferrate(III)]-4-chloropyridinium chloride. Magnetic measurements on single crystals show that the $S = {}^5/_2$ material (4-bromopyridinium)$_3Fe_2Cl_{1.3}Br_{7.7}$ orders as a canted antiferromagnet at 5.67 K, while (4-chloropyridinium)$_3Fe_2Br_9$ orders in a similar fashion at 7.96 K. Magnetic susceptibility data are compared with the theoretical predictions for the simple cubic (sc) Heisenberg high-temperature series expansion model, and superexchange pathways for the isostructural series of monoclinic $A_3Fe_2X_9$ salts are examined.

Introduction

This paper is the second in a series on some ferric compounds of stoichiometry $A_3Fe_2X_9$.[1] By comparison with a variety of other transition metal salts having this stoichiometry, one might expect to find binuclear [Fe_2X_9]$^{3-}$ ions in the crystal structure, but this has not been found to be true in these or other Fe(III) compounds of which we are aware. Rather, discrete, tetrahedral [FeX_4]$^-$ ions (X = Cl, Br) are found to be present. We report here the syntheses, the crystal structures, and the magnetic properties for the new mixed-halide compound [4-Br(py)H]$_3Fe_{1.3}Br_{7.7}$, and similar data for [4-Cl(py)H]$_3Fe_2Br_9$(4-X(py)H = 4-halo-

* To whom correspondence should be addressed at the University of Illinois at Chicago.

(1) Part 1: Zora, J. A.; Seddon, K. R.; Hitchcock, P. B.; Lowe, C. B.; Shum, D. P.; Carlin, R. L. *Inorg. Chem.*, preceding paper in this issue.

0020-1669/90/1329-3308$02.50/0